Arabian Journal of Chemistry (2015) xxx, xxx–xxx

King Saud University

Arabian Journal of Chemistry

www.ksu.edu.sa
www.sciencedirect.com

ORIGINAL ARTICLE

Elaboration and characterisation of novel low-cost adsorbents from grass-derived sulphonated lignin

Nasir M.A. Al-Lagtah [a,b,*], Alaa H. Al-Muhtaseb [c], Mohammad N.M. Ahmad [d,e], Yousef Salameh [d,e]

[a] School of Chemical Engineering and Advanced Materials, Newcastle University, Singapore 599493, Singapore
[b] School of Chemical Engineering and Advanced Materials, Newcastle University, Newcastle upon Tyne, NE1 7RU, United Kingdom
[c] Department of Petroleum and Chemical Engineering, Faculty of Engineering, Sultan Qaboos University, Muscat, Oman
[d] School of Chemistry and Chemical Engineering, Queen's University of Belfast, Belfast, United Kingdom
[e] Chemical Engineering Program, Faculty of Engineering and Architecture, American University of Beirut, Beirut, Lebanon

Received 28 November 2014; accepted 26 June 2015

KEYWORDS

Sulphonated lignin;
Chemical activation;
Surface characterisation;
Central composite design;
Response surface methodology;
Activation mechanism

Abstract This study investigated the use of water-soluble sulphonated lignin (SL) extracted from grass, which has not been used before as a precursor of activated carbon (AC). Chemical activation of SL with three dehydrating salts ($ZnCl_2$, KCl, $Fe_2(SO_4)_3{\cdot}xH_2O$) at various salt concentrations (10%, 20%, 30% w/w), charring temperatures (600, 700 °C) and charring times (1, 2 h) has been carried out. The surface characteristics and removal efficiencies of cadmium, copper and zinc ions from aqueous solutions were affected by the activation conditions. The sulphonated lignin-based activated carbons (SLACs) with the highest specific surface area, total pore and micropore volume were produced at the lowest dehydrating salt concentration (10% w/w) and at 700 °C and 2-h charring. These optimal sulphonated lignin-based ACs were named SLAC-ZC (optimal grass-derived SLAC activated by zinc chloride); SLAC-PC (optimal grass-derived SLAC activated by potassium chloride) and SLAC-FS (optimal grass-derived SLAC activated by ferric sulphate). The central composite design and surface response methodology of different SLACs characteristics showed that the optimal responses were achieved at the same operating conditions. These SLACs also achieved the highest removal efficiencies of Cd^{2+}, Cu^{2+} and Zn^{2+} ions from aqueous solutions. The chemical activation had significantly increased the total porosity, microporosity and surface area of water-soluble SL. The activation mechanism depended on the used dehydrating salt where the

* Corresponding author at: School of Chemical Engineering and Advanced Materials, Newcastle University International Singapore, 537 Clementi Road, #06-01, Singapore 599493, Singapore. Tel.: +65 6469 7053; fax: +65 6467 3473.
E-mail address: nasir.al-lagtah@newcastle.ac.uk (N.M.A. Al-Lagtah).

Peer review under responsibility of King Saud University.

Production and hosting by Elsevier

http://dx.doi.org/10.1016/j.arabjc.2015.06.033

Please cite this article in press as: Al-Lagtah, N.M.A. et al., Elaboration and characterisation of novel low-cost adsorbents from grass-derived sulphonated lignin. Arabian Journal of Chemistry (2015), http://dx.doi.org/10.1016/j.arabjc.2015.06.033

porosity developed by the dehydration effect of $ZnCl_2$, and by a series of hydrolysis and redox reactions for the other two salts. The results of this research demonstrated that water-soluble SL has a great potential as a novel precursor for the production of activated carbons.

1. Introduction

The effectiveness of adsorption on commercial activated carbon (CAC) for removal of a wide variety of contaminants from wastewater has made it an ideal alternative to other expensive treatment options. Because of its substantial adsorption capacity, CAC is considered one of the most effective adsorbents (Djati Utomo et al., 2015). Despite the fact that CACs are flexible and very efficient adsorbents, their high cost limits their use. The high cost of CAC is mainly due to the costs of its synthesis and treatments that involve high energy consumption, its low yield, or its reactivation and associated losses requiring partial replacement, up to 15% (Deliyanni et al., 2015).

The need for diminishing the cost of producing activated carbon has prompted research into finding precursors that are less expensive and widely available. These 'low-cost' alternatives must be, by definition, cheap, readily available and require little processing for activation. Industrial and agricultural wastes (such as wood, sawdust, fruit pits, cellulose, and lignin) represent potentially economical alternative precursors (Yahya et al., 2015).

Lignin is the second most abundant natural raw material and nature's most abundant aromatic (phenolic) polymer, whose main function is to fixate the cellulose fibres in plants. Lignin is a heavily cross-linked polymer and hence has great variation, even within the same plant species (Watkins et al., 2015). Lignin is generally obtained from the black liquor discharged as a waste from paper mills in large quantities (more than 50 million tons annually), which can pose a major problem of disposal. Therefore, there has been an increasing interest in the development of economically viable new applications of lignin. However, the structure and characteristics of lignin molecules differ subject to the wood or biomass species obtained from and, to an even larger degree, on the pretreatment processes used to separate them. These pretreatment processes include kraft, soda, sulphite, organosolv, and hydrolysis methods. Currently, much of the lignin is consumed as a low-grade fuel to fire pulping boilers. Although there are some other secondary applications, such as an adhesive or tanning agent, no major large scale application has so far been commercially proven. Only 1–2% of the various types of lignin are utilized in non-fuel value-added applications (Myglovets et al., 2014).

A possible application for excess lignin is as a precursor for the activated carbon production. Lignin has high carbon content and a molecular structure similar to bituminous coal, which is one of the most used precursors for AC production. One of the theories regarding the origin of bituminous coal is that lignin, not cellulose, is the parent material since the degradation of the aromatic compounds of lignin results in a complex mixture of compounds that undergo different processes to produce coal (Major, 1996; Boyce et al., 2010). Lignin has a carbon content greater than 60%, which may offer the eminent carbon yield needed for the commercial elaboration of activated carbon and can partially replace non-renewable coal-based ACs (Myglovets et al., 2014).

Activated carbon can be produced from lignin by chemical activation process, which is a single step process where carbonisation of lignin takes place in the presence of dehydrating salt that influences pyrolytic decomposition, inhibiting the formation of tar and thereby enhancing the yield and porosity of the activated carbon. The temperatures used in chemical activation process are relatively lower than those used in physical activation process (Mahmoudi et al., 2014). Lignin can be chemically activated by impregnating inactivated lignin with activating agent such as $ZnCl_2$, KCl, KOH, K_2CO_3, NaOH and H_3PO_4, followed by charring at temperatures in the range 450–900 °C, depending on the activating agent used. This method often leads to materials with higher micropore volumes and wider micropore sizes (Titirici, 2013).

Most of the published work is on the production of activated carbons from lignin investigated the use of water-insoluble kraft lignin as precursor (Myglovets et al., 2014). However, sulphonated lignin (SL) still has not been sufficiently investigated as a precursor for the production of activated carbons and there were very few publications on the use of WSSL to produce activated carbons (Cho and Susuki, 1980; Lee, 2013; Myglovets et al., 2014). SL is produced as a by-product of sulphite pulping, in which the pretreatment of wood or biomass is performed through the use of HSO_3^- and SO_3^- ions. As a result, SL is water-soluble anionic polyelectrolytes that contain a large number of charged groups. SL is commercially produced in relatively large quantities, totalling approximately 2 million tons per year as dry solids (Myglovets et al., 2014). This study addresses the major gap in investigating the visibility of activated carbon production from water-soluble SL derived from grass, which has not been used before as AC precursor. Activated carbons are chemically produced from SL using three dehydrating salts: zinc chloride ($ZnCl_2$), potassium chloride (KCl) and iron(III) sulphate ($Fe_2(SO_4)3{\cdot}xH_2O$). Up to the authors' knowledge, the last two activating agents have not been used before to produce ACs from SL. This investigation includes the study of different variables that may affect the quality of SL-based activated carbons (SLACs). These variables include: the concentration of the dehydrating salt solution, the charring temperature and time. The produced SL-based activated carbons (SLACs) are subsequently used for the removal of three heavy metal ions (Cd^{2+}, Cu^{2+} and Zn^{2+}) from aqueous solutions in order to choose the optimal SLACs.

Experimental design using response surface methodology (RSM) is a multivariate statistical technique, which is widely applied to optimise the processes and to discover the conditions in which to apply a procedure in order to obtain the best possible response in the experimental region studied. This methodology involves the design of experiments and multiple

Please cite this article in press as: Al-Lagtah, N.M.A. et al., Elaboration and characterisation of novel low-cost adsorbents from grass-derived sulphonated lignin. Arabian Journal of Chemistry (2015), http://dx.doi.org/10.1016/j.arabjc.2015.06.033

regression analysis as tools to assess the effects of two or more independent variables on dependent variables. The principal advantage of RSM is the reduced number of experimental trials needed to evaluate multiple parameters and their interactions. An additional advantage is the possibility of evaluating the interaction effect between the independent variables on the response. This technique is based on the fit of a polynomial equation to the experimental data to describe the behaviour of a set of data. In this way, a mathematical model which describes the studied process is generated. The objective is to simultaneously optimise the levels of the studied variables to attain the best possible performance of the process (Messaoud and Houas, 2015; Gil et al., 2013). Recently, RSM became a popular statistical tool for process optimisation and has been recently used for the optimisation of activated carbon production from coconut shell, bamboo waste, Turkish lignite, tamarind wood, jatropha hull and olive waste cake and date stone (Danish et al., 2014). According to the literature review conducted in this study, no previous work has been done on optimisation of ACs production from water-soluble SL by RSM, considering simultaneously as variables the concentration of the dehydrating salt solution, the charring temperature and time. Therefore, a novel objective of this work is to carry out a methodical study of the preparation conditions of chemically activated carbons from SL and its influence on the characteristics of the activated carbons. An experimental design was used for the preparation conditions of activated carbons from SL via chemical activation with three dehydrating salts and RSM was applied to optimise the experimental conditions. In this study, the built-in options of Solver and Data Analysis of Microsoft Excel®, which have not been used before in such studies, are implemented to carry out the experimental design, modelling and optimisation tasks.

2. Materials and methods

2.1. Precursor characteristics

Water-soluble SL is extracted from the liquor obtained from the pre-treatment step of grass hydrolysis process. The liquor contains substantial amounts of lignin and small quantities of other components (inorganic and organic salts, sugars). The sulphonation of lignin was carried out by firstly removing the major portion of inorganic salts, small molecules of organic salts and sugars from the liquor by acidification to a pH of approximately 3–4 with a 30% aqueous solution of sulphuric acid. Secondly, the precipitated lignin was filtered and washed to decrease its residual sulphuric acid content. The lignin slurry was finally sulphonated by adding sodium sulphite, increasing its pH from 4 to 9. This reaction was carried out in an autoclave. The bomb and contents were heated at 140 °C for about four hours under constant rotation. After cooking, the product was removed from the bomb, filtered to eliminate insoluble by-products, treated in order to reduce its sulphonate content and then dried.

2.2. Chemical activation and charring

The dehydrating salt solutions are prepared from $ZnCl_2$ (BDH AnalaR, UK), KCl and $Fe_2(SO_4)_3{\cdot}xH_2O$ salts (Sigma–Aldrich Company, UK) by mixing the correct amount of each salt with 600 mL of deionised water to obtain 10, 20 and 30% w/w stock solutions. Grass-derived sulphonated lignin is soluble in water. Therefore, a paste is formed by mixing SL and the stock solution of a dehydrating salt at an impregnation ratio of 1:1 according to the reported method by Hayashi et al. (2000). Charring of the samples took place in a muffle furnace (Carbolite LMF4, Carbolite Ltd., UK). The samples are weighed and then placed into crucibles with sealed lids to restrict air diffusion. The crucibles are placed into the furnace whilst they are at room temperature and the furnace is then set to a charring temperature of 600 or 700 °C. When the charring temperature has been reached, the samples are held at that temperature for one or two hours. At the end of charring time, the furnace is switched off and allowed to cool till it reaches room temperature. Each charred sample is washed to remove any excess chemicals, dried and then weighed to determine its yield percentage according to Eq. (1).

$$\text{Yield}(\%) = 100(w_2/w_1) \tag{1}$$

where w_1 is the initial weight of sulphonated lignin dried sample (g) and w_2 is the weight of the char red sample (g).

2.3. Physical and chemical characteristics

The surface physical characterisations of the chemically activated carbons produced the grass-derived SL include the determination of BET, external and micropore specific surface areas; total pore, micropore volumes and pore size distribution. Adsorption/desorption isotherms of N_2 are generated using a gas porosimeter (Nova 4200, Quantachrome Instruments, UK). The measured relative pressure and adsorbed volume of nitrogen gas are used in Brunauer–Emmett–Teller (BET) isotherm to calculate the total specific surface area (A_{BET}). The *t*-plot method is applied in order to estimate the micropore volume (V_{micro}), micropore specific surface area (A_{micro}) and external specific surface area (A_{ext}) for the produced SLACs. The total pore volume (V_{total}) is estimated from the volume of nitrogen held at the relative pressure $P/P_0 \approx 0.95$. The sum of mesopore and macropore volume (V_{me+ma}) is obtained by subtracting the micropore volume from the total pore volume (Al-Ghouti, 2004).

2.4. Equilibrium adsorption analysis

Batch adsorption experiments are conducted to estimate the removal efficiency of three representative heavy metals by each produced grass-derived SLAC. Aqueous solutions of three divalent heavy metals (Cd^{2+}, Cu^{2+} and Zn^{2+}) are initially prepared in a final concentration of 50 ± 5 mg L^{-1}. The equilibrium adsorption experiments are carried out in 50 cm^3 glass bottles where 25 ± 1 mg of each SLAC and 25 ± 1 cm^3 of the test adsorbate solution are mixed. The jars are sealed and constantly agitated for 96 h at room temperature whilst maintaining the shaking speed at 150 rpm. After reaching the equilibrium, the jars are removed from the shaker and the mixture is filtered to remove the adsorbent. The first portion of the filtrate is discharged to avoid the effects of metal ions adsorption on the filter paper. The filtrate is collected in polythene tubes and diluted before analysis. The initial and equilibrium concentrations of the three heavy metals are

Please cite this article in press as: Al-Lagtah, N.M.A. et al., Elaboration and characterisation of novel low-cost adsorbents from grass-derived sulphonated lignin. Arabian Journal of Chemistry (2015), http://dx.doi.org/10.1016/j.arabjc.2015.06.033

determined using inductive coupled plasma (ICP) (IRIS Intrepid, Thermo-Fisher Scientific, USA) after diluting the filtrate to an adequate concentration.

The removal percentage of each adsorbate is calculated using Eq. (2):

$$\text{Removal}(\%) = 100(C_0 - C_e)/C_0 \quad (2)$$

where C_0 and C_e (mg L^{-1}) are the liquid-phase concentration of each adsorbate at initial and equilibrium conditions, respectively.

2.5. Design of experiments and response surface methodology

Production of activated carbons from grass-derived SL is affected by various process variables, namely charring temperature (X_1), dehydrating salt concentration (X_2) and charring time (X_3). These variables determine the extent of different uncontrolled responses characterising the produced SLACs. These responses are yield (%), BET and micropore specific surface areas ($m^2\ g^{-1}$) and total pore and micropore volumes ($cm^3\ g^{-1}$). The effects and interactions of the three process variables are evaluated by central composite design (CCD) method. This method is suitable for describing each response by a second-order polynomial equation, which will help into optimising the effective process variables using response surface methodology (RSM) (Salman, 2014). Each response is correlated using the following second-order polynomial equation:

$$\text{Response} = b_o + \sum_{i=1}^{3} b_i X_i + \sum_{i=1}^{2}\sum_{j=2}^{3} b_{ij} X_i X_j + \sum_{i=1}^{3} b_{ii} X_i^2 \quad (3)$$

where b_o, b_i, b_{ii}, b_{ij} are constant, linear, quadratic and interaction coefficients, respectively, and X_i, X_j are values of the factors that may affect each response. Usually the range of each process variable is transformed into $[-1, 1]$ range of codes to build models. These codes are listed in Table 1.

The fitting and regression of each second-order polynomial equation for each response is carried out using Microsoft Excel® Solver. The best fitting is determined by applying different error functions, which are:

- The Sum of the Squares of the Errors (SSE)

This error estimation method is represented by Eq. (4):

$$\text{SSE} = \sum_{i=1}^{n} (Y_{cal} - Y_{\text{exp}})^2 \quad (4)$$

The symbol Y stands for each correlated response and the subscripts "*exp*" and "*cal*" stands for the experimental and calculated values and n is the number of observations in the experimental data. The smaller the SSE value, the better curve fitting is (Hadi et al., 2010).

Table 1 Model codes for transforming the process variables.

Process variable	Real values	Code
X_1: Charring temperature (°C)	[600, 700]	[−1, 1]
X_2: Dehydrating salt concentration (%)	[10, 20, 30]	[−1, 0, 1]
X_3: Charring time (h)	[1, 2]	[−1, 1]

- The Marquardt's Percent Standard Deviation (MPSED)

This error function is widely used in different research areas. It is similar to a geometric mean error distribution which was modified to allow for the number of degrees of freedom of the system (Ncibi, 2008). This error estimation method is represented by Eq. (5):

$$\text{MPSED}(\%) = 100 * \sqrt{\frac{1}{n-2}\sum_{i=1}^{n}\left(\frac{Y_{cal} - Y_{\text{exp}}}{Y_{\text{exp}}}\right)^2} \quad (5)$$

- Nonlinear chi-square test (χ^2)

This test is a statistical tool is used to find the best fitting of a model. It is obtained by assessing the sum of squared differences between the experimental and the calculated data, with each squared difference is divided by its corresponding value, calculated from the model, as shown in Eq. (6):

$$\chi^2 = \sum_{i=1}^{n} \frac{(Y_{cal} - Y_{\text{exp}})^2}{Y_{cal}} \quad (6)$$

3. Results and discussion

3.1. Elaboration of activated carbons from grass-derived SL

Grass-derived water-soluble SL was used as a precursor for the production of ACs. The BET specific surface area, total pore volume and the average pore size of the grass-derived SL are 9.76 $m^2\ g^{-1}$, 0.00787 $cm^3\ g^{-1}$ and 1.59 nm, respectively. Three different dehydrating salts at three different concentrations were used to produce activated carbons under charring conditions as detailed in Section 2.2. The produced SLACs were in a granular form since the preparation process led to the formation of a paste, which due to the chemical activation, broke into granules with a mean size around 1.0 mm. The produced SLACs were also insoluble in water, which is an advantage of chemical activation of water-soluble SL.

3.1.1. The yield of grass-derived SLACs

The final yield of the 27 SLACs decreased as the charring temperature increased, as illustrated in Fig. 1, regardless of the used dehydrating salt. On the other hand, increasing the dehydrating salt concentration from 10% to 30% w/w slightly increased the yield. Such small increase in the yield indicates that no further volatilization took place after that all volatile matters have been removed in the first stage of charring process (El Qada et al., 2008).

The highest yield was achieved when SL was activated by $ZnCl_2$, followed by KCl and finally by $Fe_2(SO_4)_3{\cdot}xH_2O$. It is expected that $ZnCl_2$ to give the highest yield since zinc chloride promotes the decomposition of carbonaceous material during the charring process, restricts the formation of tar and thusly increases the carbon yield (Uçar et al., 2009).

3.1.2. The surface characteristics of grass-derived SLACs

3.1.2.1. BET, external and micropore specific surface areas. The BET, external and micropore specific surface areas of the 27 SLACs are shown in Fig. 2. The surface area decreased with increasing the dehydrating salt concentration regardless of the charring temperature or time. Moreover, increasing the charring time from 1 to 2 h at charring temperature of 600 °C increased the surface area. Therefore, the two-hour

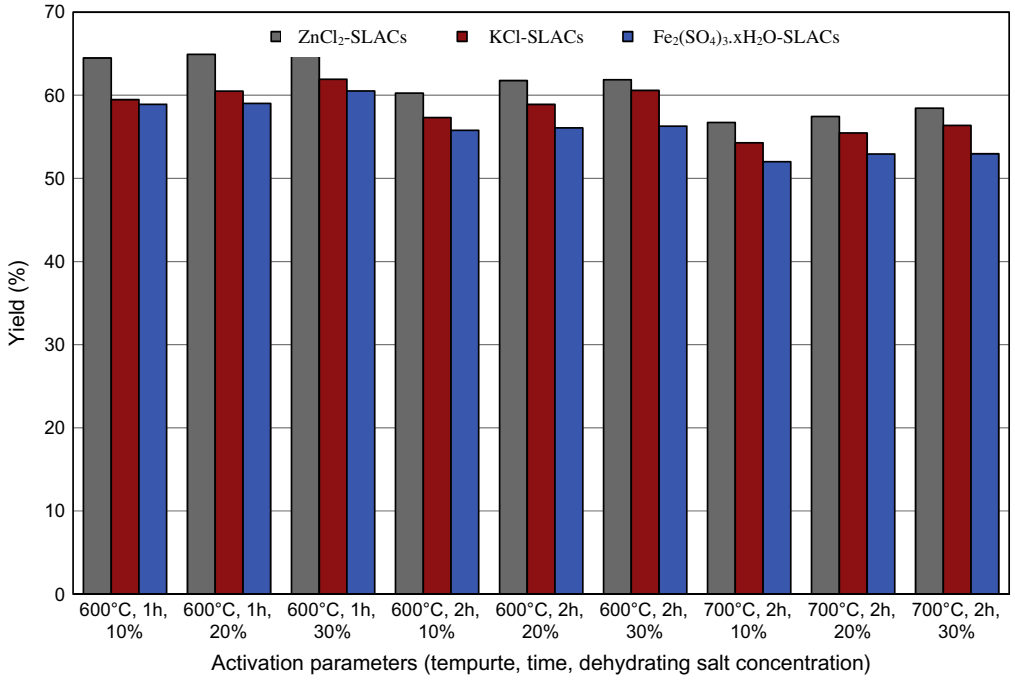

Figure 1 Effect of final charring temperature, time and dehydrating salt concentration on the yield of sulphonated lignin-based activated carbons at impregnation ratio of 1:1.

period of charring was chosen for the higher charring temperature of 700 °C and this choice proved to be successful since BET specific surface area increased further.

For $ZnCl_2$-SLACs, the amount of zinc introduced into the precursor during the impregnation was the prime factor governing the change in their specific surface areas. The change of KCl concentration was also the key factor affecting the specific surface area of KCl-SLACs. For $Fe_2(SO_4)_3{\cdot}xH_2O$-SLACs, increasing the charring temperature and time was the dominant factors affecting their specific surface areas.

Cho and Susuki (1980) extracted sodium sulphonated lignin from pulp mill sludge and used it as a precursor of ACs using $ZnCl_2$ as activating agent. Their results showed that increasing the charring temperature generally increased their A_{BET}. On the other hand, their reported yields decreased as the charring temperature increased.

El Qada et al. (2008) used the same three dehydrating salts for activating bituminous coal but at different charring temperatures (400, 600, 800 and 900 °C) and times (1, 4 and 6 h). The authors noted that increasing the charring temperature and time would generally increase their A_{BET} and V_{total}. They also found that A_{BET} decreased as the dehydrating salt concentration increased and they found as well that the magnitude of A_{BET} specific was in the order of $ZnCl_2$-ACs > KCl-ACs > $Fe_2(SO_4)_3{\cdot}xH_2O$-ACs, which is the same order observed in this study.

3.1.2.2. Total pore and micropore volumes. The total pore volume of the 27 produced SLACs is shown in Fig. 3. The increase in dehydrating salt concentration caused a decrease in V_{total}. On the other hand, increasing the charring time from 1 to 2 h at 600 °C increased V_{total} and when the two-hour period of charring was applied at 700 °C, V_{total} increased further.

The change in V_{total} of SLACs is dependent on the applied dehydrating salt. For $ZnCl_2$-SLACs, the increase of charring time from 1 to 2 h at 600 °C and 10% w/w led to an increase in V_{total}. However at 20% and 30% w/w, the increase of charring time at 600 °C had almost no effect. Finally, the increase of charring temperature from 600 to 700 °C almost doubled the value of V_{total}. Regarding KCl-SLACs and $Fe_2(SO_4)_3{\cdot}xH_2O$HH-SLACs, the main factor affecting the value of V_{total} was mainly controlled by the charring temperature.

Fig. 4 shows the values of V_{micro} and V_{me+ma} of the 27 produced SLACs. The V_{micro} for all produced SLACs decreased with the increase of dehydrating salt concentration, which was also true regarding A_{micro} (see Fig. 2). The shrinkage of the micropores would be due to the increase in dehydrating salt concentration. For $ZnCl_2$-SLACs, the values of V_{me+ma} at 600 °C and 1 or 2 h reduced when $ZnCl_2$ concentration increased. However, when the charring temperature increased from 600 to 700 °C, V_{me+ma} value increased as $ZnCl_2$ concentration increased. The reason would be that V_{total} of $ZnCl_2$-$SLAC_2$ at 700 °C was almost constant, ranging from 0.55 to 0.57 $cm^3\ g^{-1}$ and with the decrease in V_{micro}, the sum of mesopore and macropore volume would increase. However, for the other two dehydrating salts, V_{me+ma} values did not show similar trend.

3.2. Removal of heavy metal ions from aqueous solutions

The produced SLACs were used for the removal of Cd^{2+}, Cu^{2+} and Zn^{2+} from aqueous solutions. The final removal percentages of Cd^{2+}, Cu^{2+} and Zn^{2+} from aqueous solutions by different sulphonated lignin-based ACs are represented in Fig. 5.

Please cite this article in press as: Al-Lagtah, N.M.A. et al., Elaboration and characterisation of novel low-cost adsorbents from grass-derived sulphonated lignin. Arabian Journal of Chemistry (2015), http://dx.doi.org/10.1016/j.arabjc.2015.06.033

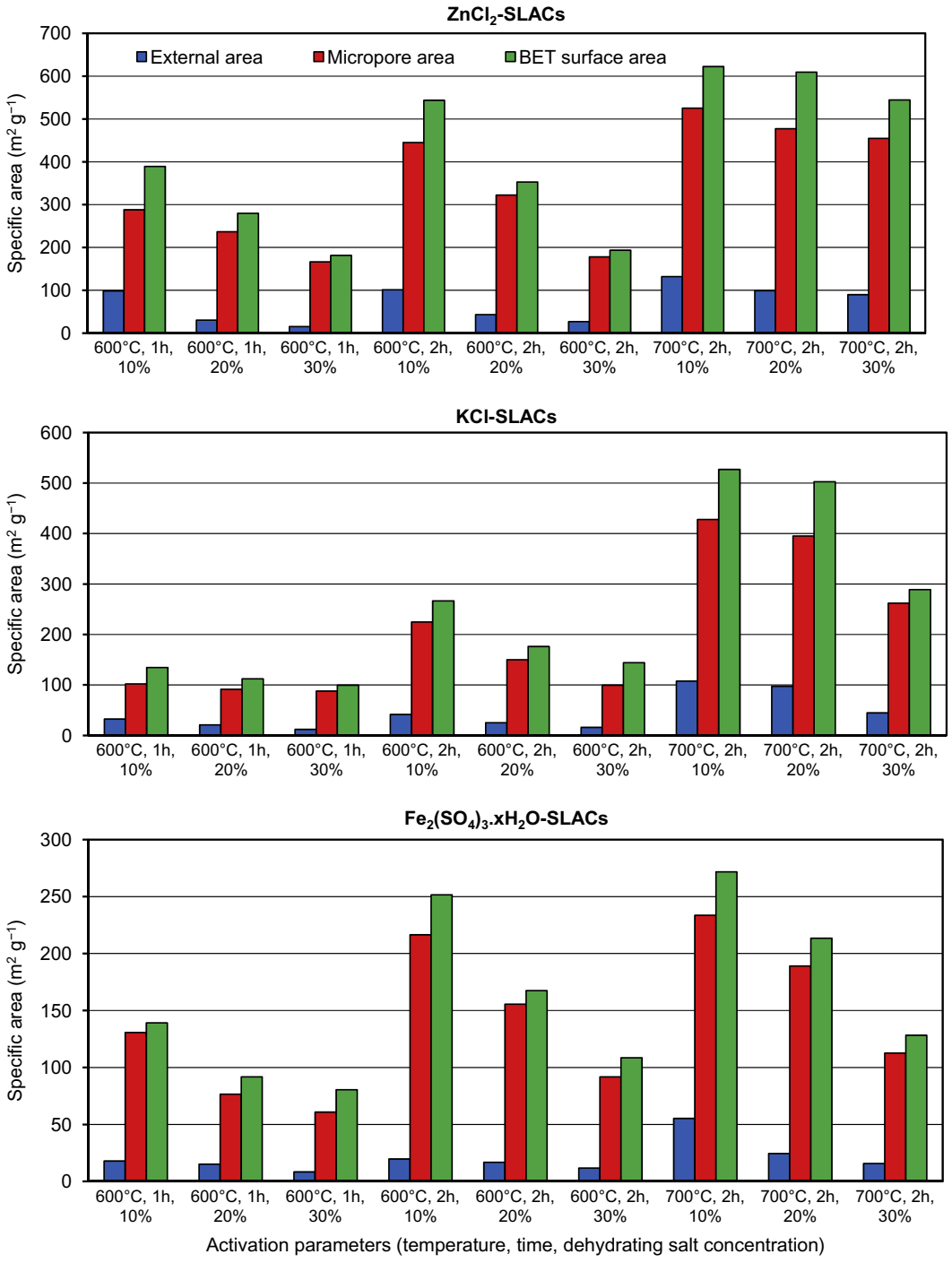

Figure 2 Effect of final charring temperature, time and dehydrating salt concentration on the specific areas of sulphonated lignin-based activated carbons at impregnation ratio of 1:1.

The maximum removal percentage of the three metal ions was achieved by SLACs prepared at 10% w/w dehydrating salt concentration, 700 °C and 2 h. The following table summarises the maximum removal percentages for the three metal ions.

As the maximum A_{BET} for each group of produced SLACs had been achieved under these conditions, it could be assumed that the extent of heavy metal removal was totally related to the magnitude of A_{BET} of each grass-derived SLAC. Therefore, these three SLACs were assumed to be the optimal produced SLACs and named SLAC-ZC (optimal grass-derived SLAC activated by zinc chloride); SLAC-PC (optimal grass-derived SLAC activated by potassium chloride) and SLAC-FS (optimal grass-derived SLAC activated by ferric sulphate). The highest removal percentage for the three metal ions was achieved by SLAC-ZC which has the largest A_{BET} as shown in Table 2. The magnitude of A_{BET} was in the following order:

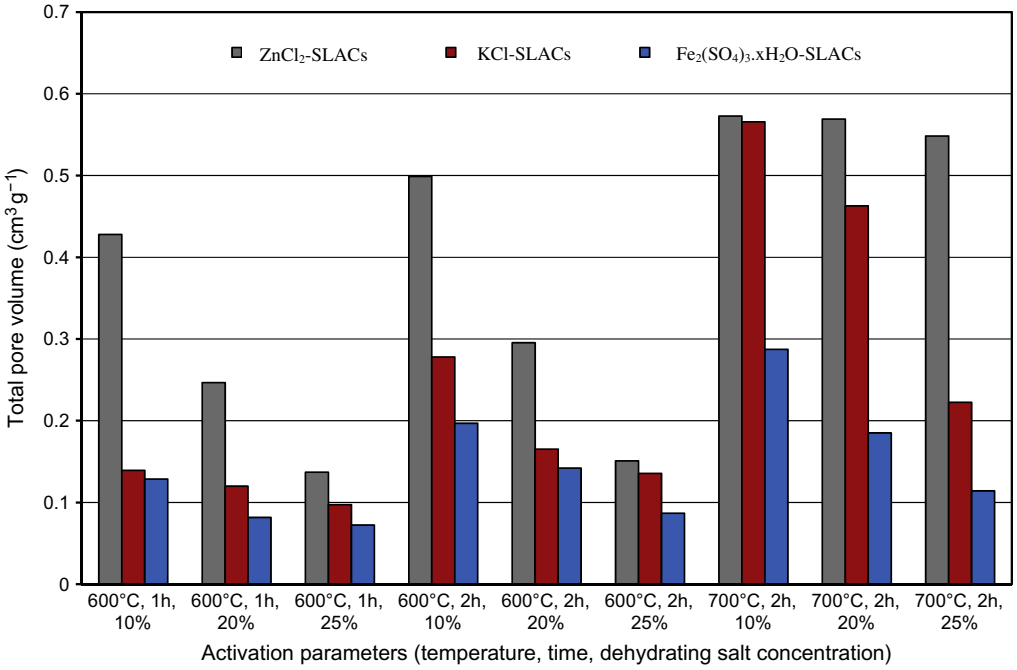

Figure 3 Effect of final charring temperature, time and dehydrating salt concentration on the specific pore volumes of sulphonated lignin-based activated carbons at impregnation ratio of 1:1.

SLAC-ZC > SLAC-PC > SLAC-FS and it could be observed that the final removal percentage for each metal ion followed the same order.

Comparing the values of the different specific surface areas (Table 3) and pore volumes (Table 4) of the precursor (grass-derived SL) and its optimal produced SLACs showed a substantial increase after chemical activation. A_{BET} of the precursor (grass-derived SL) is less than $10\,m^2\,g^{-1}$ but it had increased considerably after chemical activation by 64 times for SLAC-ZC, 54 times for SLAC-PC and 28 times for SLAC-IS. Additionally, the total pore volume of the precursor (grass-derived SL) is very low and the chemical activation has increased it significantly by 73 folds for SLAC-ZC, 72 folds for SLAC-PC and 37 folds for SLAC-IS. On the other hand, it seemed that most of the pore volume of grass-derived SL consisted of micropores (64.7% of the total pore volume). However, the value of micropore volume is very low, which indicates that there are not many voids and intraparticle channels. Once more, the chemical activation of the precursor (grass-derived SL) has increased its microporosity. All these observations would confirm that chemical activation of grass-derived SL is very beneficial.

3.3. Central composite design (CCD) and response surface methodology (RSM)

This section contains the models describing the different responses (yield, A_{BET}, A_{micro}, V_{total}, V_{micro}) as functions of different process variables (charring temperature (X_1), dehydrating salt concentration (X_2) and charring time (X_3)). The best fitting of all responses was achieved by minimising nonlinear chi square test, which also resulted in minimising the other two error functions. The adequacy of the models was further justified through single-factor analysis of variance (ANOVA) using the data analysis option provided by Microsoft Excel®. The *F*-value of each model was significant and its *P*-value was less than 5% proving that significance of model regression at 95% confidence level. However, when the each term of the model was analysed further using ANOVA, some of them were insignificant since their *P*-values were greater than 5%. Therefore, the models presented in this section only contain the significant terms.

The optimal coded second-order polynomials for the response of the yield of grass-derived SLACs are shown in Table 5, along with the ranges of experimental and estimated values and the values of chi square test and correlation coefficient. It can be noticed that the interaction coefficients between X_2 (dehydrating salt concentration) and the other two process variables are insignificant to all the yield responses of grass-derived SLACs. Moreover, the term (X_2^2) is also insignificant for the yield response of $Fe_2(SO_4)3{\cdot}xH_2O$-SLACs.

The responses of different terms are not additive properties and hence not all the variables are independent (Sheha et al., 2013). Some terms have positive sign indicating synergistic effect (i.e. direct proportionality between the variables and responses), whilst others have negative sign indicating antagonistic effect (i.e. inverse proportionality between the variables and responses) (Salman, 2014). The yield's responses for all grass-derived SLACs show that it increases with increasing the dehydrating salt concentration (positive sign of X_2 term), whilst it decreases with increasing the charring temperature and time (negative signs of X_1 and X_3 terms). These observations support the conclusions obtained from interpolating the experimental data in Fig. 1.

For BET surface area and micropores surface area responses for all the grass-derived SLACs are shown in Tables 6 and 7, respectively. There is no obvious trend of which terms are significantly affecting these two responses.

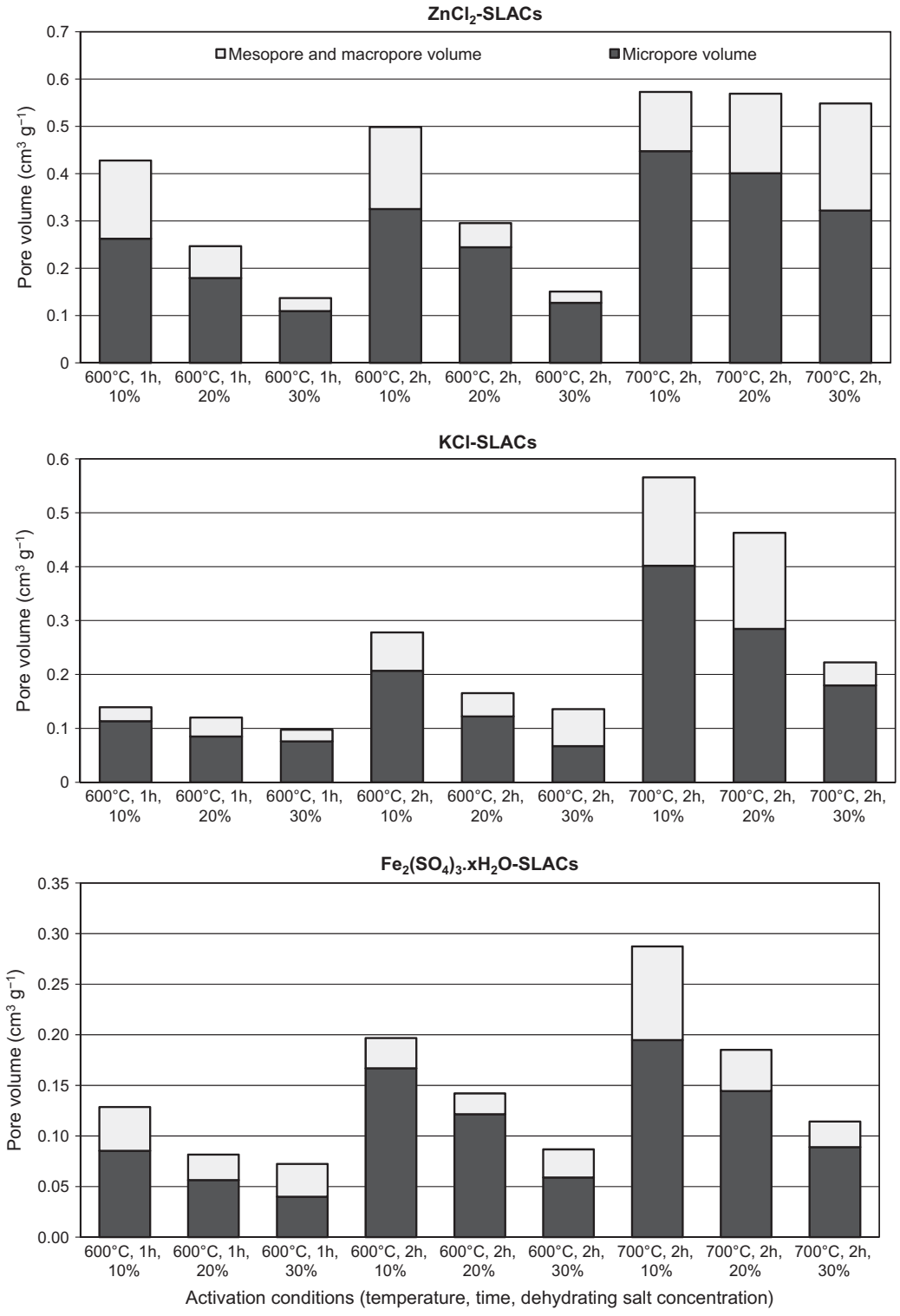

Figure 4 Effect of final charring temperature, time and dehydrating salt concentration on the specific mesopore and micropore volumes of sulphonated lignin-based activated carbons at impregnation ratio of 1:1.

However, the term X_2^2 is insignificant for all the grass-derived SLACs. Once more, the effect of dehydrating salt concentration was almost negligible to the responses of A_{BET} and A_{micro}. However, the effect of X_2 was significant and inversely proportional to the response of A_{micro} of all grass-derived SLACs.

The two responses of A_{BET} and A_{micro} increase with increasing the charring temperature and time and when the effect of dehydrating salt concentration is significant, their responses decrease as the concentration increases. All that confirm the observations concluded from the depicted data in Fig. 2. Finally, the interaction between the charring temperature

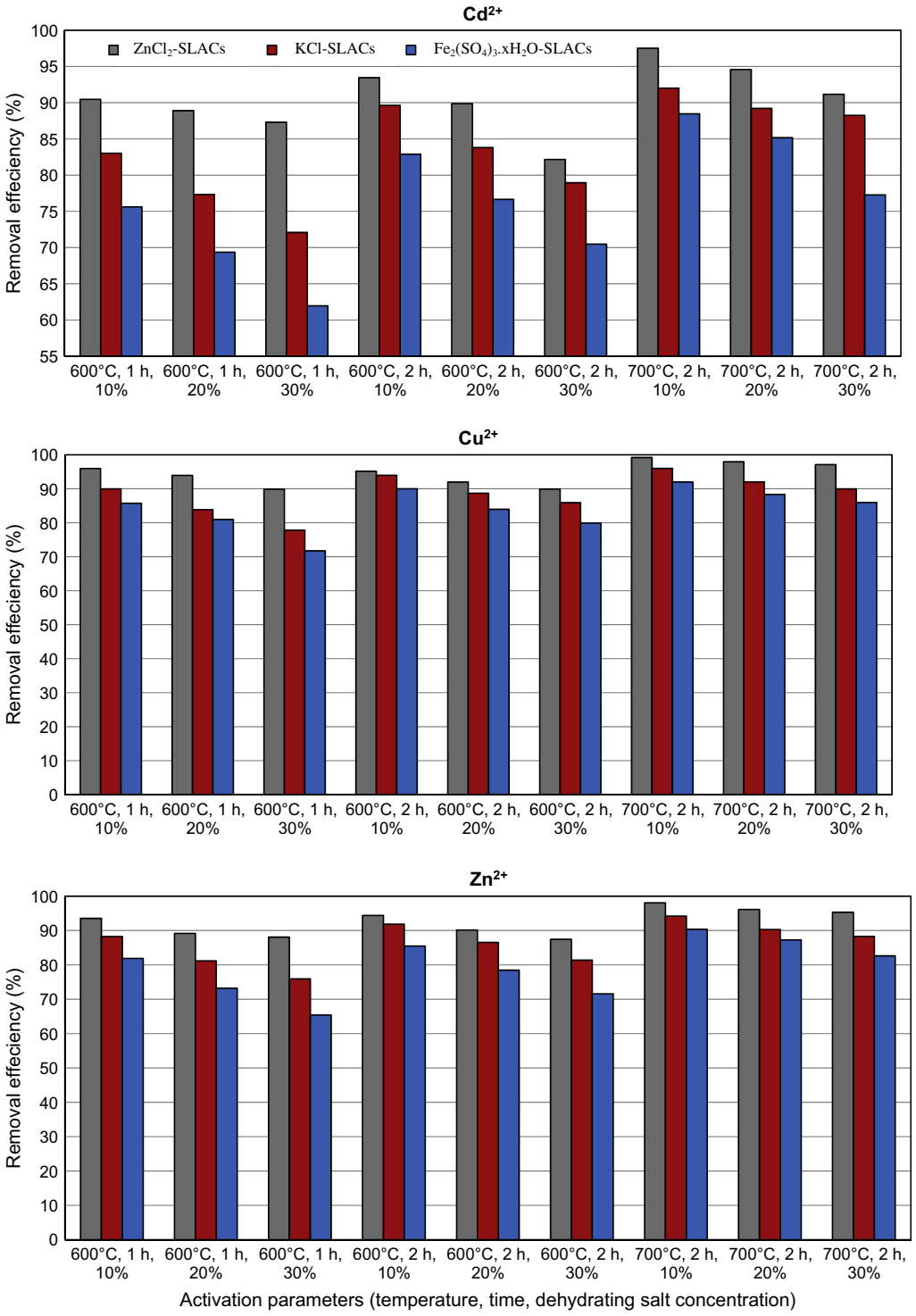

Figure 5 Removal percentage of Cu^{2+}, Cd^{2+} and Zn^{2+} by different chemically activated carbons from sulphonated lignin at different charring temperatures, time and dehydrating salts concentrations.

and time (i.e. X_1X_3 term) is significant on the two responses and they are dependent and directly proportional.

The models for the responses of the total pore and micropore volume for all grass-derived SLACs are shown in Tables 8 and 9, respectively.

The responses of V_{total} and V_{micro} can be divided into two categories: the responses for $ZnCl_2$-SLACs on one hand and for both KCl-SLACs and $Fe_2(SO_4)_3{\cdot}xH_2O$-SLACs on the other. For $ZnCl_2$-SLACs, the only two insignificant terms were X_2X_3 and X_2^2. The pore volumes increase with the increase of charring temperature and time, whilst they decrease as the dehydrating salt concentration increases. Also, the interactions between charring temperature and the other two process variables are significant and positively signed, indicating direct

Table 2 Maximum final removal percentages of Cd^{2+}, Cu^{2+} and Zn^{2+} by optimal grass-derived sulphonated lignin-based activated carbons (SLACs).

Grass derived SL-based activated carbon	Activation condition	BET surface area ($m^2\ g^{-1}$)	Average pore size (nm)	Heavy metal final removal percentage		
				Cd^{2+}	Cu^{2+}	Zn^{2+}
SLAC-ZC	Salt concentration: 10% (w/w)	622.5	1.85	97.5	99.2	98.1
SLAC-PC	(700 °C, 2 h)	527.1	1.91	92.0	96.0	94.2
SLAC-FS		271.7	1.99	88.5	92.0	90.4

Table 3 Total pore, micropore and mesopore volumes and average pore size of optimal grass-derived SLACs and grass-derived SL.

	SLAC-ZC	SLAC-PC	SLAC-IS	Grass-derived SL
A_{BET} ($m^2\ g^{-1}$)	622.5	527.1	271.7	9.760
A_{micro} ($m^2\ g^{-1}$)	525.2	427.8	233.6	8.192
% of A_{BET}	84.4	81.2	86.0	83.9
A_{ext} ($m^2\ g^{-1}$)	132.0	107.6	55.2	1.568
% of A_{BET}	21.2	20.4	20.3	16.1

Table 4 BET, micropore and external specific surface areas of optimal grass-derived SLACs and grass-derived SL.

	SLAC-ZC	SLAC-PC	SLAC-IS	Grass-derived SL
V_{total} ($cm^3\ g^{-1}$)	0.5728	0.5657	0.2874	7.869E−3
V_{micro} ($cm^3\ g^{-1}$)	0.4474	0.4017	0.1947	5.093E−3
% of V_{total}	78.1	71.0	67.7	64.7

proportionality. These observations confirm the conclusions realized from Fig. 3.

On the other hand, the responses of pore volumes of the other two groups of SLACs have three insignificant terms (X_1X_2, X_2X_3 and X_2^2). Also, these responses decrease with the increase of charring temperature and dehydrating salt concentration but increase as the charring time increases. The only significant interaction term is between charring temperature and time. Finally and contradictory to the responses of $ZnCl_2$-SLACs pore volumes, the signs of the second-order terms are negative.

The calculated values of different responses using CCD method are compared to the experimental values for different grass-derived SLACs and shown in Appendix A. The calculated values for all the responses of $ZnCl_2$-SLACs are very similar to their experimental values. For KCl-SLACs, the comparison between experimental and calculated values for the responses of A_{micro}, V_{total} and V_{micro} is scattered and shows higher difference compared to the responses of *Yield* and A_{BET}. Finally, the calculated responses for $Fe_2(SO_4)_3{\cdot}xH_2O$-SLACs are different than the experimental values but without a clear trend and the differences are smaller than those of KCl-SLACs.

3.3.1. Process optimisation

All the responses of specific surface areas and pore volumes are optimised using Microsoft Excel® solver. The optimal predicted values of each response are found at charring temperature of 700 °C, dehydrating salt concentration of 10% w/w and charring time of two hours. These optimal conditions are exactly similar to the conditions that gave the highest removal efficiencies of the three heavy metals. Also, the highest experimental values of A_{BET}, A_{micro}, V_{total} and V_{micro} were achieved at these conditions. A comparison between the experimental and predicted values is given in Table 10. The absolute relative error between the experimental and predicted values for different responses ranged from 0.5% to 22.7%. The predicted values for the responses of $ZnCl_2$-SLACs were all higher than the experimental values, whilst they were lower than the experimental values for the other two groups of SLACs except for A_{BET}.

The figures of selected response surface methodology (RSM) for the yield, A_{BET} and V_{total} of the different grass-derived SLACs are shown in Appendix B. The novelty of these figures comes from the use Microsoft Excel® 3-D surface chart option.

4. Proposed activation mechanisms

Zinc chloride is widely used to activate organic precursors based on its dehydrating function and thus alters the carbonisation behaviour of precursor. During the process of activation, $ZnCl_2$ combines hydrogen and oxygen atoms within the organic materials to water, resulting in the generation of porosity as well as enhancing the carbon content. $ZnCl_2$ gets intercalated into the carbon matrix by impregnation. Upon carbonisation, the impregnated $ZnCl_2$ causes dehydration of the carbon precursor leading to charring and aromatization

Table 5 The optimal coded second-order models for the response of the yield of grass-derived SLACs.

Grass derived SL-based activated carbons	CCD model	Experimental range of yield	Calculated range of yield	Chi square test χ^2	Correlation coefficient R^2
Response: yield (%)					
$ZnCl_2$-SLACs	$\text{Yield} = 56.71 - 1.888X_1 + 0.787X_2 - 1.889X_3 + 0.003X_1X_3 + 2.33X_1^2 - 0.114X_2^2 + 2.33X_3^2$	56.7–65.8	56.6–65.7	5.82×10^{-3}	0.996
KCl-SLACs	$\text{Yield} = 56.65 - 1.951X_1 + 1.297X_2 - 0.674X_3 + 0.179X_1X_3 + 0.586X_1^2 + 0.584X_3^2$	54.3–61.9	54.1–61.9	7.19×10^{-3}	0.992
$Fe_2(SO_4)_3{\cdot}xH_2O$-SLACs	$\text{Yield} = 54.72 - 1.94X_1 + 0.508X_2 - 1.481X_3 + 0.232X_1X_3 + 0.557X_1^2 + 0.543X_3^2$	52.0–60.5	52.1–60.0	1.29×10^{-2}	0.990

Table 6 The optimal coded second-order models for the response of BET surface area of grass-derived SLACs.

Grass derived SL-based activated carbon	CCD model	Experimental range of BET surface area	Calculated range of BET surface area	Chi square test χ^2	Correlation coefficient R^2
Response: BET surface area ($m^2\,g^{-1}$)					
$ZnCl_2$-SLACs	$A_{BET} = 439.0 + 125.1X_1 - 114.5X_2 + 29.7X_3 + 0.633X_1X_3 + 0.59X_1^2 + 0.59X_3^2$	181.6–622.5	181.0–632.4	1.26	0.916
KCl-SLACs	$A_{BET} = 225.4 + 90.13X_1 + 69.82X_3 - 34.53X_1X_2 + 30.23X_1X_3 + 9.917X_1^2 + 9.917X_3^2$	99.7–527.1	98.2–562.4	15.8	0.967
$Fe_2(SO_4)_3{\cdot}xH_2O$-SLACs	$A_{BET} = 136.0 + 21.16X_1 + 49.22X_3 - 14.72X_1X_2 + 17.9X_1X_3 + 0.591X_1^2 + 0.591X_3^2$	80.5–271.7	62.1–277.6	16.3	0.936

Please cite this article in press as: Al-Lagtah, N.M.A. et al., Elaboration and characterisation of novel low-cost adsorbents from grass-derived sulphonated lignin. Arabian Journal of Chemistry (2015), http://dx.doi.org/10.1016/j.arabjc.2015.06.033

Table 7 The optimal coded second-order models for the response of the micropore surface area of grass-derived SLACs.

Grass derived SL-based activated carbon	CCD model	Experimental range of micropore surface area	Calculated range of micropore surface area	Chi square test χ^2	Correlation coefficient R^2
Response: micropore surface area ($m^2\,g^{-1}$)					
$ZnCl_2$-SLACs	$A_{micro} = 357.7 + 91.96X_1 - 79.61X_2 + 37.24X_3 + 0.63X_1X_3 - 17.98X_2X_3 + 0.59X_1^2 + 0.59X_3^2$	166.4–525.2	167.4–518.7	0.564	0.928
KCl-SLACs	$A_{micro} = 218.0 + 98.55X_1 - 36.36X_2 + 29.72X_3 + 1.608X_1X_3 + 0.745X_1^2 + 3.094X_3^2$	87.7–427.8	58.8–388.1	45.9	0.937
$Fe_2(SO_4)_3{\cdot}xH_2O$-SLACs	$A_{micro} = 131.7 + 11.42X_1 - 48.51X_2 + 29.79X_3 + 1.0.633X_1X_3 + 0.593X_1^2 + 0.593X_3^2$	60.9–233.6	43.8–223.2	14.7	0.955

Table 8 The optimal coded second-order models for the response of the total pore volume of grass-derived SLACs.

Grass derived SL-based activated carbon	CCD model	Experimental range of total pore volume	Calculated range of total pore volume	Chi square test χ^2	Correlation coefficient R^2
Response: total pore volume ($m^3\,g^{-1}$)					
$ZnCl_2$-SLACs	$V_{total} = 0.146 + 0.054X_1 - 0.082X_2 + 0.09X_3 + 0.069X_1X_2 + 0.074X_1X_3 + 0.1X_1^2 + 0.099X_3^2$	0.137–0.573	0.135–0.583	1.60×10^{-3}	0.997
KCl-SLACs	$V_{total} = 0.172 - 0.229X_1 - 0.061X_2 + 0.355X_3 + 0.322X_1X_3 - 0.122X_1^2 - 0.122X_3^2$	0.097–0.566	0.062–0.437	0.118	0.867
$Fe_2(SO_4)_3{\cdot}xH_2O$-SLACs	$V_{total} = 0.117 - 0.293X_1 - 0.049X_2 + 0.336X_3 + 0.315X_1X_3 - 0.145X_1^2 - 0.145X_3^2$	0.072–0.287	0.048–0.234	2.81×10^{-2}	0.900

Please cite this article in press as: Al-Lagtah, N.M.A. et al., Elaboration and characterisation of novel low-cost adsorbents from grass-derived sulphonated lignin. Arabian Journal of Chemistry (2015), http://dx.doi.org/10.1016/j.arabjc.2015.06.033

Table 9 The optimal coded second-order models for the response of the micropore volume of grass-derived SLACs.

Grass derived SL-based activated carbon	CCD model	Experimental range of micropore volume	Calculated range of micropore volume	Chi square test χ^2	Correlation coefficient R^2
Response: micropore volume ($m^3\ g^{-1}$)					
$ZnCl_2$-SLACs	$V_{micro} = 0.120 + 0.038X_1 - 0.075X_2 + 0.064X_3 + 0.012X_1X_2 + 0.043X_1X_3 + 0.063X_1^2 + 0.062X_3^2$	0.109–0.447	0.107–0.451	1.19×10^{-3}	0.997
KCl-SLACs	$V_{micro} = 0.166 - 0.234X_1 - 0.051X_2 + 0.322X_3 + 0.307X_1X_3 - 0.145X_1^2 - 0.145X_3^2$	0.076–0.402	0.045–0.323	5.47×10^{-2}	0.906
$Fe_2(SO_4)_3{\cdot}xH_2O$-SLACs	$V_{micro} = 0.089 - 0.306X_1 - 0.038X_2 + 0.343X_3 + 0.32X_1X_3 - 0.154X_1^2 - 0.154X_3^2$	0.040–0.195	0.026–0.177	1.87×10^{-2}	0.939

Table 10 Comparison between experimental and predicted values of different responses of grass-derived SLACs.

Response	Grass-derived SLACs								
	$ZnCl_2$-SLACs			KCl-SLACs			$Fe_2(SO_4)_3{\cdot}xH_2O$-SLACs		
	Experimental value	Predicted value	Relative error (%)	Experimental value	Predicted value	Relative error (%)	Experimental value	Predicted value	Relative error (%)
A_{BET} ($m^2\ g^{-1}$)	622.5	709.7	−14.0	527.1	562.4	−6.70	271.7	277.6	−2.15
A_{micro} ($m^2\ g^{-1}$)	525.2	586.3	−11.6	427.8	388.1	9.29	233.6	223.2	4.45
V_{total} ($cm^3\ g^{-1}$)	0.573	0.576	−0.50	0.566	0.437	22.7	0.287	0.234	18.7
V_{micro} ($cm^3\ g^{-1}$)	0.447	0.453	−1.35	0.402	0.323	19.5	0.195	0.177	9.09

Please cite this article in press as: Al-Lagtah, N.M.A. et al., Elaboration and characterisation of novel low-cost adsorbents from grass-derived sulphonated lignin. Arabian Journal of Chemistry (2015), http://dx.doi.org/10.1016/j.arabjc.2015.06.033

along with the creation of pores. During the process of activation, mobile liquid $ZnCl_2$ is formed above the melting point (283 °C). Further increase in the temperature of charring, around and beyond the boiling point of $ZnCl_2$ (730 °C), allows interaction between carbon atoms and Zn species resulting in a significant widening of the interlayers of carbon, creating pores in the carbon matrix. During such severe interactions with carbon, $ZnCl_2$ aids removal of water from carbon structure by stripping off hydrogen and oxygen of the organic precursor (Viswanathan et al., 2009). Therefore, increasing activating temperature to 700 °C will insure the stripping of water, creating of highly porous structure and hence increasing the specific surface areas and pore volumes. Such observation is confirmed since the highest specific surface areas and pore volumes of $ZnCl_2$-SLACs are achieved at 700 °C, as shown in Figs. 2–4.

The chemical activation mechanism of grass-derived sulphonated lignin by KCl and $Fe_2(SO_4)_3{\cdot}xH_2O$ is different. The first step of their activation mechanism is hydrolysis of these two salts and then the products of these hydrolysis reactions will develop the carbon porosity by a series of redox reactions (Fleming et al., 2010; Ningrum, 1990; Wang et al., 2014).

For KCl activation mechanism, the first step is the hydrolysis reaction:

$$KCl + H_2O \rightarrow KOH + HCl \quad (22)$$

The potassium hydroxide will activate grass-derived sulphonated lignin by a series of redox reactions where the carbon content is oxidized to CO, CO_2 and carbonate, whilst KOH is reduced into K_2CO_3 or metallic potassium (Wang et al., 2014). The general redox reaction of KOH and carbon content of sulphonated lignin can be written as follows:

$$4KOH + l \rightarrow K_2CO_3 + K_2O + 2H_2 \quad (23)$$

The breakdown of KOH into K_2O occurs along with the reduction of carbon that takes place during the activation process through the additional reactions. One of these reactions involves generating steam that will prompt the removal of unstructured carbon as CO, leading to formation of pores. In other reactions, additional carbon is utilized, reducing K^+ to K. All these carbon losses cause the formation of porous structure. Therefore, the KCl activation mechanism consists of hydrolysis step; activating grass-derived sulphonated lignin with steam as well as with K_2CO_3 (Guo et al., 2002). The effectiveness of KCl activation of grass-derived sulphonated lignin can be attributed to the capacity of K to intercalate into the lamella of the carbon crystallites without difficulty, which will widen the space between the adjacent carbon layers (intercalation phenomenon), resulting in an increase in the specific surface area. In addition, the formation, penetration and the reduction of *in-situ* K_2O to elemental K by carbon result in carbon gasification with a subsequent emission of CO_2 leading to the formation of pores. Moreover, K atoms that intercalate into the lamella of the carbon crystallites widen the space between the adjacent carbon layers (intercalation phenomenon), resulting in an increase in the value of specific surface area (Ji et al., 2007).

The effect of charring temperature on KCl activation process can be divided into two steps. The first step is a pre-activation step at charring temperatures less than 300 °C, during which KCl is hydrolysed to produce a new activating agent (i.e. KOH). The potassium hydroxide is then dehydrated, followed by structure transformation, but virtually no pores are developed. The second step is an activation step at charring temperatures greater than 550 °C since the process of pore development demands a large amount of activation energy. However, the charring temperatures between 300 and 550 °C cause the depolymerisation of sulphonated lignin, leading to the development of a number of micropores. The higher charring temperatures will result in widening the pores. As a result, some of the micropores are converted to mesopores. If the charring temperature is increased above 800 °C, the mesopores will be widened further, causing a reduction in the specific surface area of produced SLAC (Tian et al., 2011).

Shen and Xue (2003) noticed that increasing KOH concentration up to 8% w/w (~11% w/w KCl concentration) would increase the specific surface areas of the produced ACs due to the extensive gasification of carbon content along with the development of porosity, which was mainly because of the micropore widening process. Such pore widening process resulted in the production of micro- and mesoporous activated carbons. However, increasing the activating agent above 8% w/w (~11% w/w KCl concentration) caused the collapse of pore wall and the loss of mesoporosity and hence reducing the specific surface area. That would relate well to the interpolation of the illustrated data of KCl-SLACs in Figs. 2 and 4 where the increase in KCl concentration caused a decrease in specific surface areas and the micropore volumes, regardless of the charring temperature and time.

The activation mechanism of ferric sulphate has not been investigated thoroughly before. However, the effect of temperature and acidity on the hydrolysis of ferric sulphate has been well investigated as part of ferric ion extraction from iron ores. At high temperatures (>200 °C) and low acidity, ferric sulphate is hydrolysed producing ferric oxide as follows (Huang et al., 2014):

$$Fe_2(SO_4)_3 \cdot xH_2O + 3H_2O \rightarrow Fe_2O_3 + 3H_2SO_4 + xH_2O \quad (24)$$

The use of ferric oxide (Fe_2O_3) as an oxygen carrier to enhance the gasification of coal and biomass has drawn major interest because of its low cost and its ability to act as a catalyst for decomposing and reforming the undesirable production of tar (Huang et al., 2014). Therefore, it can be assumed that during the activation of grass-derived sulphonated lignin at elevated temperatures (600 and 700 °C), ferric sulphate is hydrolysed to Fe_2O_3, which will activate the carbon content through redox reactions. The activation can occur through two redox routes.

The first route is the oxidization of carbon by steam produced from the hydrolysis reaction, generating carbon monoxide that will be oxidized further by ferric oxide as follows:

$$2CO + 4Fe_2O_3 \rightarrow 2CO_2 + 2Fe_3O_4 + 2FeO \quad (25)$$

The new produced iron oxide will act as an oxygen carrier and hence will improve the charring by minimising the formation of tar by cracking it into hydrogen, carbon monoxide and hydrocarbons.

The second route is the overall redox reaction between carbon and ferric oxide:

$$2C + Fe_2O_3 \rightarrow CO + CO_2 + Fe_3O_4 + FeO \quad (26)$$

In summary, these redox routes will play two roles in grass-derived sulphonated lignin activation. On one hand, the utilization of intermediate products (i.e. CO, H_2) will speed up the charring process and therefore improve the porosity of

Please cite this article in press as: Al-Lagtah, N.M.A. et al., Elaboration and characterisation of novel low-cost adsorbents from grass-derived sulphonated lignin. Arabian Journal of Chemistry (2015), http://dx.doi.org/10.1016/j.arabjc.2015.06.033

the produced activated carbon. On the other hand, the reaction products (i.e. H_2O, CO_2) can function as activating agents enhancing further the charring and the produced activated carbon's porosity.

5. Conclusion

Grass-derived sulphonated lignin (SL) showed a great potential as novel precursor for the development of activated carbon by using three dehydrating salts: $ZnCl_2$, KCl and $Fe_2SO_4{\cdot}xH_2O$ at three different concentrations (10%, 20% and 30% w/w), two charring temperatures (600 and 700 °C) and two charring periods (one and two hours). The final yield of the produced grass-derived SL-based activated carbons (SLACs) decreased as the charring temperature increased, whilst increasing the dehydrating salt concentration increased it marginally. The increase in the initial dehydrating salt concentration generally decreased BET, external and micropore specific surface areas. At charring temperature of 600 °C, increasing the charring period from one to two hours increased the surface area. Therefore, the two-hour charring period was selected for charring temperature of 700 °C. At such conditions, the surface areas were the highest. Similar trends were noticed regarding the total pore and micropore volumes.

The increase in A_{BET} resulted in an increase in the final removal percentage of three heavy metals (Cd^{2+}, Cu^{2+} and Zn^{2+}) from aqueous solutions. Therefore the SLACs produced at 10% w/w dehydrating salt concentration, 700 °C and 2 h were selected as the optimal grass-derived SLACs. These three adsorbents were named as SLAC-ZC, SLAC-PC and SLAC-IS. The A_{BET} of the precursor (grass-derived SL) had increased considerably after chemical activation by 64 times for SLAC-ZC, 54 times for SLAC-PC and 28 times for SLAC-IS.

The central composite design for the responses of A_{BET}, A_{micro}, V_{total} and V_{micro} for the 27 produced grass-derived SLACs showed that the effect of different process variables and their interaction were not all significant. Based on the use of ANOVA analysis, the responses were modelled using second-order polynomial equations and the process was optimised to find the optimal value for each response, which was achieved at the same process variables for the optimal experimental values.

Sulphonated lignin is usually considered as a waste stream of paper industry or biomass pre-treatment processes with limited industrial applications. This study showed useful and profitable application of sulphonated lignin in the field of activated carbon synthesis.

Appendix A. Supplementary material

Supplementary data associated with this article can be found, in the online version, at http://dx.doi.org/10.1016/j.arabjc.2015.06.033.

References

Al-Ghouti, M.A., 2004. Mechanisms and Chemistry of Dye Adsorption on Diatomite and Modified Diatomite (Ph.D. thesis). Queen's University of Belfast, Belfast, UK. doi: http://dx.doi.org/10.1016/j.jhazmat.2009.11.059.

Boyce, C.K., Abrecht, M., Zhou, D., Gilbert, P.U.P.A., 2010. X-ray photoelectron emission spectromicroscopic analysis of arborescent lycopsid cell wall composition and Carboniferous coal ball preservation. Int. J. Coal Geol. 83, 146–153. http://dx.doi.org/10.1016/j.coal.2009.10.008.

Cho, B.R., Susuki, M., 1980. Activated carbon by pyrolysis of sludge pulp-mill waste-water treatment. J. Chem. Eng. Jpn. 13, 463–467.

Danish, M., Hashim, R., Mohamad Ibrahim, M.N., Sulaiman, O., 2014. Optimized preparation for large surface area activated carbon from date (Phoenix dactylifera L.) stone biomass. Biomass Bioenergy 61, 167–178. http://dx.doi.org/10.1016/j.biombioe.2013.12.008.

Deliyanni, E.A., Kyzas, G.Z., Triantafyllidis, K.S., Matis, K.A., 2015. Activated carbons for the removal of heavy metal ions: a systematic review of recent literature focused on lead and arsenic ions. Open Chem. 13 (1), 699–708. http://dx.doi.org/10.1515/chem-2015-0087.

Djati Utomo, H., Natalie Phoon, R.Y., Shen, Z., Ng, L.H., Lim, Z.B., 2015. Removal of methylene blue using chemically modified sugarcane bagasse. Nat. Resour. 6, 209–220. http://dx.doi.org/10.4236/nr.2015.64019.

El Qada, E., Allen, S.J., Walker, G., 2008. Influence of preparation conditions on the characteristics of activated carbons produced in laboratory and pilot scale systems. Chem. Eng. J. 142, 1–13. http://dx.doi.org/10.1016/j.cej.2007.11.008.

Fleming, C.A., Brown, J.A., Botha, M., 2010. An economic and environmental case for re-processing gold tailings in South Africa. In: 42nd Annual Meeting of the Canadian Mineral Processors Proceedings, Ottawa, Canada.

Gil, M.V., Martínez, M., García, S., Rubiera, F., Pis, J.J., Pevida, C., 2013. Response surface methodology as an efficient tool for optimizing carbon adsorbents for CO_2 capture. Fuel Process. Technol. 106, 55–61. http://dx.doi.org/10.1016/j.fuproc.2012.06.018.

Guo, Y., Yang, S., Yu, K., Zhao, J., Wang, Z., Xu, H., 2002. The preparation and mechanism studies of rice husk based porous carbon. Mater. Chem. Phys. 74, 320–323. http://dx.doi.org/10.1016/S0254-0584(01)00473-4.

Hadi, M., Samarghandi, M.R., McKay, G., 2010. Equilibrium two-parameter isotherms of acid dyes sorption by activated carbons: study of residual errors. Chem. Eng. J. 160, 408–416. http://dx.doi.org/10.1016/j.cej.2010.03.016.

Hayashi, J., Kazehaya, A., Muroyama, K., Watkinson, A.P., 2000. Preparation of activated carbon from lignin by chemical activation. Carbon 38, 1873–1878. http://dx.doi.org/10.1016/S0008-6223(00)00027-0.

Huang, Z., He, F., Feng, Y., Liu, R., Zhao, K., Zheng, A., Chang, S., Zhao, Z., Li, H., 2014. Characteristics of biomass gasification using chemical looping with iron ore as an oxygen carrier. Int. J. Hydrogen Energy 38, 14568–14575. http://dx.doi.org/10.1016/j.ijhydene.2013.09.022.

Ji, Y., Li, T., Li, Z., Wang, X., Lin, Q., 2007. Preparation of activated carbons by microwave heating KOH activation. Appl. Surf. Sci. 254, 506–512. http://dx.doi.org/10.1016/j.apsusc.2007.06.034.

Lee, D., 2013. Preparation of a sulfonated carbonaceous material from lignosulfonate and its usefulness as an esterification catalyst. Molecules 18, 8168–8180. http://dx.doi.org/10.3390/molecules18078168.

Mahmoudi, K., Hamdi, N., Srasra, E., 2014. Preparation and characterization of activated carbon from date pits by chemical activation with zinc chloride for methyl orange adsorption. J. Mater. Environ. Sci. 5 (6), 1758–1769.

Major, T., 1996. Genesis and the Origin of Coal and Oil, second ed. Apologetics Press Inc., Montgomery, USA.

Messaoud, J.B., Houas, A., 2015. Preparation of activated carbon from residues coffee by physical activation: using Response surface methodology. Int. J. Adv. Res. 3 (3), 1025–1033.

Myglovets, M., Poddubnaya, O.I., Sevastyanova, O., Lindström, M.E., Gawdzik, B., Sobiesiak, M., Tsyba, M.M., Sapsay, V.I., Klymchuk, D.O., Puziy, A.M., 2014. Preparation of carbon adsorbents from lignosulfonate by phosphoric acid activation for the adsorption of metal ions. Carbon 771–783. http://dx.doi.org/10.1016/j.carbon.2014.09.032.

Ncibi, M.C., 2008. Applicability of some statistical tools to predict optimum adsorption isotherm after linear and non-linear regression analysis. J. Hazard. Mat. 153 (1–2), 207–212. http://dx.doi.org/10.1016/j.jhazmat.2007.08.038.

Ningrum, N.S., 1990. The Production of Activated Carbon from Indonesian Coals for Water Treatment (Master thesis). University of Wollongong, Australia.

Salman, J.M., 2014. Optimization of preparation conditions for activated carbon from palm oil fronds using response surface methodology on removal of pesticides from aqueous solution. Arab. J. Chem. 7, 101–108. http://dx.doi.org/10.1016/j.arabjc.2013.05.033.

Sheha, D., Khalaf, H., Daghestani, N., 2013. Experimental design methodology for the preparation of activated carbon from sewage sludge by chemical activation process. Arab. J. Sci. Eng. 38, 2941–2951. http://dx.doi.org/10.1007/s13369-012-0470-4.

Shen, Z., Xue, R., 2003. Preparation of activated mesocarbon microbeads with high mesopore content. Fuel Process. Technol. 84, 95–103. http://dx.doi.org/10.1016/S0378-3820(03)00050-X.

Tian, Y., Liu, P., Wang, X., Zhong, G., Chen, G., 2011. Offgas analysis and pyrolysis mechanism of activated carbon from bamboo sawdust by chemical activation with KOH. J. Wuhan Uni. Technol. Mater. Sci. Ed. 26, 10–14. http://dx.doi.org/10.1007/s11595-011-0157-9.

Titirici, M. (Ed.), 2013. Sustainable Carbon Materials from Hydrothermal Processes. John Wiley & Sons Ltd., Chichester, UK.

Uçar, S., Erdem, M., Tay, T., Karagöz, S., 2009. Preparation and characterization of activated carbon produced from pomegranate seeds by $ZnCl_2$ activation. Appl. Surf. Sci. 255, 8890–8896. http://dx.doi.org/10.1016/j.apsusc.2009.06.080.

Viswanathan, B., Neel, P., Varadarajan, T.K., 2009. Methods of Activation and Specific Applications of Carbon Materials, National Centre for Catalysis Research, Department of Chemistry. Indian Institute of Technology Madras, Chennai, India.

Wang, S., Tristan, F., Minami, D., Fujimori, T., Cruz-Silva, R., Terrones, M., Takeuchi, K., Teshima, K., Rodríguez-Reinoso, F., Endo, M., Kaneko, K., 2014. Activation routes for high surface area graphene monoliths from graphene oxide colloids. Carbon 76, 220–231. http://dx.doi.org/10.1016/j.carbon.2014.04.071.

Watkins, D., Nuruddin, Md., Hosur, M., Tcherbi-Narteh, A., Jeelani, S., 2015. Extraction and characterization of lignin from different biomass resources. J. Mater. Res. Technol. 4 (1), 26–32. http://dx.doi.org/10.1016/j.jmrt.2014.10.009.

Yahya, M.A., Al-Qodah, Z., Zanariah Ngah, C.W., 2015. Agricultural bio-waste materials as potential sustainable precursors used for activated carbon production: a review. Renew. Sust. Energy Rev. 46, 218–235. http://dx.doi.org/10.1016/j.rser.2015.02.051.

Please cite this article in press as: Al-Lagtah, N.M.A. et al., Elaboration and characterisation of novel low-cost adsorbents from grass-derived sulphonated lignin. Arabian Journal of Chemistry (2015), http://dx.doi.org/10.1016/j.arabjc.2015.06.033